IOP Conf. Series: Journal of Physics: Conf. Series **833** (2017) 012018 doi:10.1088/1742-6596/833/1/012018

Superconductivity-induced shift of phonon frequency in the system with itinerant and strongly correlated electrons

Teet Örd, Kadri Veende, Küllike Rägo

Institute of Physics, University of Tartu, W. Ostwaldi Str. 1, 50411 Tartu, Estonia

E-mail: teet.ord@ut.ee

Abstract. We investigate a system consisting of strongly correlated localized and itinerant electron states mixed by optical vibration. The linear vibronic interaction causes the softening of active optical mode and it may induce a structural instability. The modification of renormalized phonon frequency by the gap in the energy of itinerant electrons in the superconducting phase has been established. The disposition of the electron spectrum and chemical potential influences substantially the corresponding effect. It is demonstrated that the presence of van Hove singularity in the center of itinerant electron band introduces qualitative changes into the superconductivity-induced shifts of phonon frequency.

1. Introduction

The mutual influence between superconductivity and phonon dynamics, including structural instability, has been an object of research for many years, see review [1] for earlier publications in this field. A number of effects related to the phonon dynamics, structural instabilities and symmetry breaking present in high temperature superconductors [2, 3] have been investigated intensively both experimentally and theoretically. In particular, various aspects of phonon self-energy effects caused by superconductivity were analyzed in Refs. [4, 5, 6, 7].

In the present contribution we study the changes in phonon frequency, renormalized by the vibronic mixing of itinerant and strongly correlated localized electron states, due to the electron pairing gap in the spectrum of itinerant electrons in the superconducting phase. In the absence of superconductivity, the model was examined in Ref. [8] and the special case of such a scheme was considered as a possible reason for the tetragonal-orthorhombic transition in $La_{2-x}M_xCuO_4$ [9, 10]. The vibronic hybridization of electron states has been accepted as quite general mechanism for structural (ferroelectric) phase transitions [11, 12].

2. Basic equations

We use the following model Hamiltonian for the electron-phonon system:

$$H = H_0 + H_{\mathrm{el-ph}}\,, \quad H_0 = H_{\mathrm{el}} + H_{\mathrm{ph}}\,, \quad H_{\mathrm{el}} = H_{\mathrm{l}} + H_{\mathrm{i}}\,, \tag{1}$$

$$H_{\mathrm{l}} = \sum_j \left(\varepsilon_1 \sum_s X_j^{ss} + \varepsilon_2 X_j^{22} \right)\,, \tag{2}$$

$$H_{\rm i} = \sum_{\mathbf{k}} \sum_{s} \tilde{\varepsilon}(\mathbf{k}) a^{+}_{\mathbf{k}s} a_{\mathbf{k}s} + \Delta_{\rm sc} \sum_{\mathbf{k}} a^{+}_{\mathbf{k}\uparrow} a^{+}_{-\mathbf{k}\downarrow} + \Delta^{*}_{\rm sc} \sum_{\mathbf{k}} a_{-\mathbf{k}\downarrow} a_{\mathbf{k}\uparrow} \,, \tag{3}$$

$$H_{\rm ph} = \sum_{\mathbf{q}} \hbar\omega_{\mathbf{q}} \left(b^{+}_{\mathbf{q}} b_{\mathbf{q}} + \frac{1}{2} \right) , \tag{4}$$

$$H_{\rm el-ph} = N_0^{-1} \sum_{\mathbf{k}} \sum_{j} \sum_{s} \sum_{\mathbf{q}} g(\mathbf{q}) {\rm e}^{i(\mathbf{k}-\mathbf{q})\mathbf{r}_j} a^{+}_{\mathbf{k}s} \left[X^{0s}_j + \eta(s) X^{-s2}_j \right] \left(b^{+}_{-\mathbf{q}} + b_{\mathbf{q}} \right) + {\rm h.c.}\,. \tag{5}$$

Here $H_{\rm el}$ is the Hamiltonian of electron subsystem containing localized strongly correlated electrons (Hamiltonian $H_{\rm l}$) and itinerant superconducting band electrons (Hamiltonian $H_{\rm i}$), $H_{\rm ph}$ is the Hamiltonian of phonon subsystem and $H_{\rm el-ph}$ describes the vibronic mixing of localized and itinerant electron states. In the case of localized electrons the one-electron annihilation and creation operators have been replaced by the Hubbard operators: $d_{js} = X^{0s}_j + \eta(s) X^{-s2}_j$ and $d^{+}_{js} = X^{s0}_j + \eta(s) X^{2-s}_j$ where j is the index of lattice site, s is the spin index and $\eta(\uparrow,\downarrow) = \pm 1$. In the Hamiltonian (2), $\varepsilon_1 = \varepsilon_d - \mu$ and $\varepsilon_2 = 2\varepsilon_d + U - 2\mu$ where ε_d is the energy of a localized electron without Coulomb correlation, $U/2$ is the energy of Coulomb interaction between two electrons per one spin direction and μ is the chemical potential. In the Hamiltonian (3), $\tilde{\varepsilon}(\mathbf{k}) = \varepsilon(\mathbf{k}) - \mu$, $\varepsilon(\mathbf{k})$ is the energy of an itinerant electron in the normal state and $\Delta_{\rm sc}$ is the s-wave superconductivity gap. The Hamiltonian (3) can be diagonalized by means of the Bogoliubov-Valatin transformation $a_{\mathbf{k}s} = u_{\mathbf{k}} A_{\mathbf{k}s} + v^{*}_{\mathbf{k}} A^{+}_{-\mathbf{k}-s}$.

For the energy of normal-state itinerant electrons we use the two-dimensional spectrum $\varepsilon(k_x, k_y) = -2t[\cos(k_x a) + \cos(k_y a)]$, where a is the constant of square lattice. The bottom of the energy band $\varepsilon_{\rm min} = -4t$ and the top of the band $\varepsilon_{\rm max} = 4t$. The corresponding density of electron states $\rho(\varepsilon)$ reflects the presence of van Hove singularity in the center of the band, see figure 1.

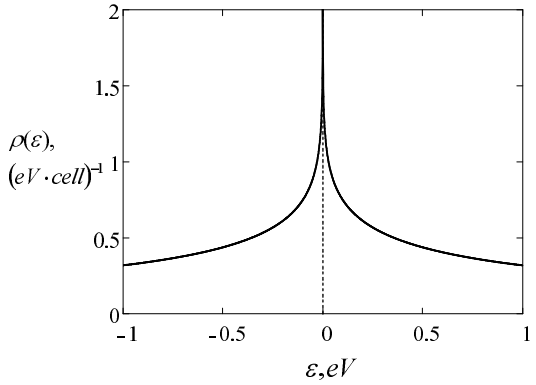

Figure 1. The density of states for the energy band of itinerant electrons with $t = 0.25\,eV$.

3. Renormalized phonon frequency

One can find the renormalized squared phonon frequency by applying the Shrieffer-Wolff transformation [13], generalized for the case of phonon-mediated dynamic hybridization between itinerant and localized electron states, to the Hamiltonian (1).

We will consider the disposition of electron states where the band of itinerant electrons is located between the lower Hubbard (LH) and upper Hubbard (UH) levels, i.e. $\varepsilon_d < \varepsilon_{\rm min}$ and $\varepsilon_d + U > \varepsilon_{\rm max}$, see figure 2. Note also that such a set of electron states is roughly similar

to the effective electron spectrum in copper-oxide systems [14, 15] stemming from the Emery model [16, 17]. Chemical potential intersects the conduction band of itinerant electrons. In what follows, we neglect the contributions containing AA, A^+A^+, X^{02}, X^{20}, $A_s^+A_{s'}$ and $X^{ss'}$ if $s \neq s'$ as well as $X_jX_{j'}$ if $j \neq j'$. Then, by introducing the average numbers of elementary excitations and electrons, one obtains for the squared phonon frequency renormalized by electron-phonon interaction

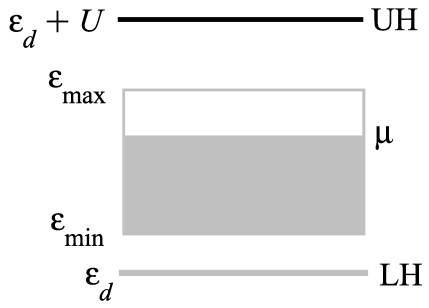

Figure 2. The configuration of electron states used.

$$\Omega_{\mathbf{q}}^2 = \omega_{\mathbf{q}}^2 + \frac{2\left|V(\mathbf{q})\right|^2}{N_0} \times \sum_{\mathbf{k}} \left\{ \frac{1}{2}\left[1 + \frac{\tilde{\varepsilon}(\mathbf{k})}{E(\mathbf{k})}\right] \left[\frac{\nu(\mathbf{k})\left(2n_0 + n_1\right) - n_1}{E(\mathbf{k}) - \varepsilon_1} + \frac{2n_2 - \nu(\mathbf{k})\left(n_1 + 2n_2\right)}{\varepsilon_2 - \varepsilon_1 - E(\mathbf{k})} \right] + \frac{1}{2}\left[1 - \frac{\tilde{\varepsilon}(\mathbf{k})}{E(\mathbf{k})}\right] \left[\frac{\nu(\mathbf{k})\left(2n_0 + n_1\right) - 2n_0}{E(\mathbf{k}) + \varepsilon_1} + \frac{\nu(\mathbf{k})\left(n_1 + 2n_2\right) - n_1}{\varepsilon_2 - \varepsilon_1 + E(\mathbf{k})} \right] \right\}, \tag{6}$$

where

$$V(\mathbf{q}) = g(\mathbf{q})\sqrt{2\omega_{\mathbf{q}}/\hbar}\,, \quad E(\mathbf{k}) = \sqrt{\tilde{\varepsilon}^2(\mathbf{k}) + |\Delta_{\mathrm{sc}}|^2}\,,$$
$$\nu(\mathbf{k}) = \left\langle A_{\mathbf{k}s}^+ A_{\mathbf{k}s} \right\rangle_{H_0}, \quad n_0 = N_0^{-1} \sum_j \left\langle X_j^{00} \right\rangle_{H_0},$$
$$n_1 = N_0^{-1} \sum_j \sum_s \left\langle X_j^{ss} \right\rangle_{H_0}, \quad n_2 = N_0^{-1} \sum_j \left\langle X_j^{22} \right\rangle_{H_0}. \tag{7}$$

It has been assumed that $\varepsilon_{\min} - \varepsilon_d \gg \hbar\omega_{\mathbf{q}}$ and $\varepsilon_d + U - \varepsilon_{\max} \gg \hbar\omega_{\mathbf{q}}$ in Eq. (6).

In the case $T = 0$ the average numbers $\nu(\mathbf{k}) = n_0 = n_2 = 0$, $n_1 = 1$ and we have for the squared frequency (6) the expression

$$\Omega_{\mathbf{q}}^2 = \omega_{\mathbf{q}}^2 - \frac{2\left|V(\mathbf{q})\right|^2}{N_0} \sum_{\mathbf{k}} \left\{ \frac{1}{2}\left[1 + \frac{\tilde{\varepsilon}(\mathbf{k})}{E(\mathbf{k})}\right] \frac{1}{E(\mathbf{k}) - \varepsilon_1} + \frac{1}{2}\left[1 - \frac{\tilde{\varepsilon}(\mathbf{k})}{E(\mathbf{k})}\right] \frac{1}{\varepsilon_2 - \varepsilon_1 + E(\mathbf{k})} \right\}, \tag{8}$$

Further, we will analyze the superconductivity-induced shift of squared phonon frequency at zero temperature

$$\frac{\Delta\Omega^2}{\omega^2} = \frac{\Omega^2 - \Omega_{\mathrm{n}}^2}{\omega^2}\,, \tag{9}$$

where $\omega \equiv \omega_{\mathbf{q}}$, $\Omega \equiv \Omega_{\mathbf{q}}$ and Ω_{n} is the value of Ω if $\Delta_{\mathrm{sc}} = 0$.

4. Numerical results and discussion

4.1. Density of electron states with van Hove singularity

By introducing the integration over the energy of itinerant electrons we can represent the squared phonon frequency (8) in the form

$$\frac{\Omega^2}{\omega^2} = 1 - \chi \int_{-4t}^{4t} \mathcal{G}(\varepsilon) \left\{ \frac{1}{2}\left[1 + \frac{\tilde{\varepsilon}(\varepsilon)}{E(\varepsilon)}\right] \frac{1}{E(\varepsilon) - \varepsilon_1} + \frac{1}{2}\left[1 - \frac{\tilde{\varepsilon}(\varepsilon)}{E(\varepsilon)}\right] \frac{1}{\varepsilon_2 - \varepsilon_1 + E(\varepsilon)} \right\} \mathrm{d}\varepsilon \,, \qquad (10)$$

where

$$\chi = \frac{2|V|^2}{\omega^2 \pi^2 t} \,, \quad \mathcal{G}(\varepsilon) = h_+^{-1}(\varepsilon) K\left(\frac{h_-(\varepsilon)}{h_+(\varepsilon)}\right) \,, \quad h_\pm(\varepsilon) = 1 \pm \left|\frac{\varepsilon}{4t}\right| \,, \qquad (11)$$

and $K(m)$ is the complete elliptic integral of the first kind.

The superconductivity-induced shifts $\Delta\Omega^2/\omega^2$ as the functions of chemical potential position are shown in figures 3, 4 for various dispositions of Hubbard levels. In the figures the energy of lower Hubbard leval ε_d is fixed and the energy of the higher Hubbard level $\varepsilon_d + U$ is tuned by the variation of U.

In figure 3 the value $U = 3\,eV$ corresponds to the symmetric location of the Hubbard levels with regard to conduction band. In this case the curve $\Delta\Omega^2/\omega^2$ *vs* μ is also symmetric, see thick broken line in figure 3. The increase of U in figure 3 introduces moderate asymmetry for the location of the Hubbard levels. As a result the strong dependence $\Delta\Omega^2/\omega^2$ *vs* μ appears in the center of conduction band ($\mu = 0$) related to the presence of van Hove singularity accompanied by the asymmetry of the function $\Delta\Omega^2(\mu)$ in the domains $\mu < 0$ and $\mu > 0$. One can observe in figure 3 that $\Delta\Omega^2(\mu) > 0$, i.e. superconductivity induces here the hardening of phonon dynamics which is, however, suppressed in the region $\mu > 0$ by the increase of U. If the chemical potential approaches the edges of conduction band, the effect of hardening increases.

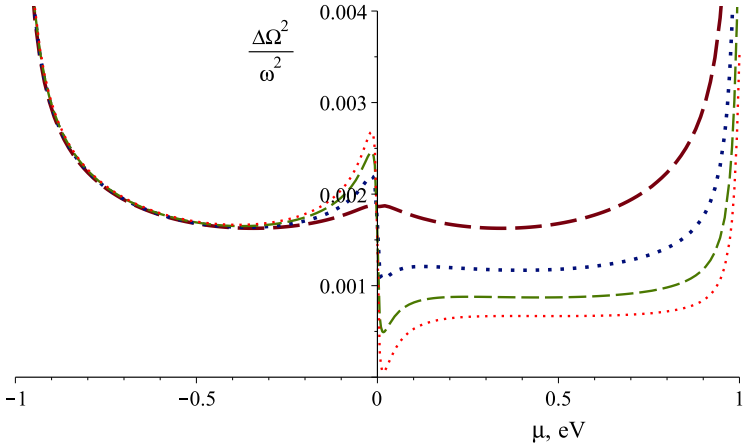

Figure 3. The dependence of $\Delta\Omega^2/\omega^2$ on μ for $U = 3\,eV$ (thick broken line), $3.25\,eV$ (thick dotted line), $3.5\,eV$ (thin broken line), $3.75\,eV$ (thin dotted line). Parameters: $\chi = 1$, $t = 0.25\,eV$, $\varepsilon_d = -1.5\,eV$, $|\Delta_{sc}| = 0.02\,eV$.

The dependence of $\Delta\Omega^2/\omega^2$ on the position of chemical potential in the case of the larger values of U is depicted in figure 4. Here the rapid fall of $\Delta\Omega^2/\omega^2$ if the increasing μ passes through the van Hove singularity leads to the softening of phonon dynamics in the domain

$\mu > 0$, see especially thin full line and thin chain line. The softening may appear also if the chemical potential approaches the top of the band of itinerant electrons (thin full line and thin chain line in figure 4).

One can follow the tendencies demonstrated in figures 3,4 also in the functions $\Delta\Omega^2/\omega^2$ *vs* U for various values of μ sown in figure 5. In particular, one can distinguish the regions of the values of μ where $\Delta\Omega^2/\omega^2$ increases or decreases with the increase of U.

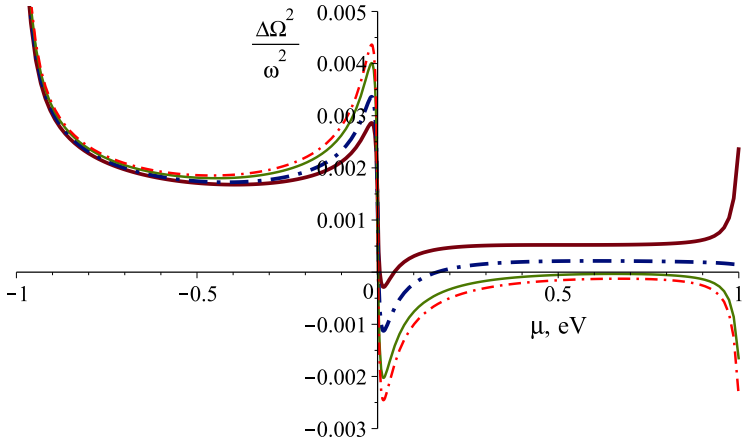

Figure 4. The dependence of $\Delta\Omega^2/\omega^2$ on μ for $U = 4\,eV$ (thick full line), $5\,eV$ (thick chain line), $8\,eV$ (thin full line), $13\,eV$ (thin chain line). For the rest of the parameters see figure 3

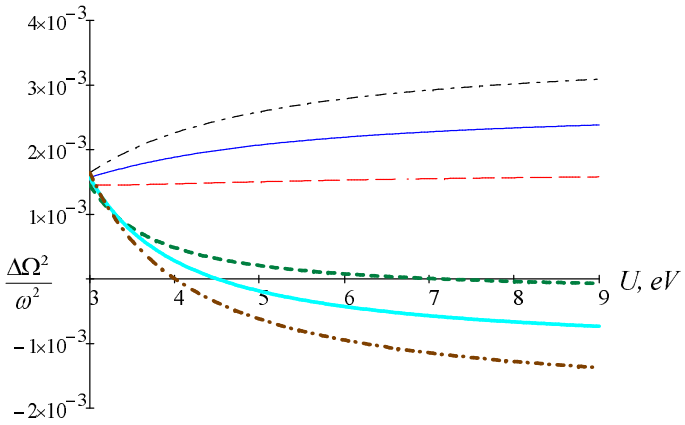

Figure 5. The dependence of $\Delta\Omega^2/\omega^2$ on U for $\mu = -0.4\,eV$ (thin broken line), $-0.1\,eV$ (thin full line), $-0.05\,eV$ (thin chain line), $0.05\,eV$ (thick chain line), $0.1\,eV$ (thick full line), $0.4\,eV$ (thick broken line). For the rest of the parameters see figure 3

4.2. Constant density of electron states

To illustrate more precisely the role of van Hove singularity in the superconductivity-induced shift of phonon frequency, we will consider for the comparison a model where the density of

itinerant electron states $\rho = \text{const}$. In this case Eq. (10) must be replaced by the expression

$$\frac{\Omega^2}{\omega^2} = 1 - \kappa \int_{\varepsilon_{\min}}^{\varepsilon_{\max}} \left\{ \frac{1}{2} \left[1 + \frac{\tilde{\varepsilon}(\varepsilon)}{E(\varepsilon)} \right] \frac{1}{E(\varepsilon) - \varepsilon_1} + \frac{1}{2} \left[1 - \frac{\tilde{\varepsilon}(\varepsilon)}{E(\varepsilon)} \right] \frac{1}{\varepsilon_2 - \varepsilon_1 + E(\varepsilon)} \right\} \mathrm{d}\varepsilon \qquad (12)$$

with $\kappa = 2|V|^2\rho/N_0\omega^2$.

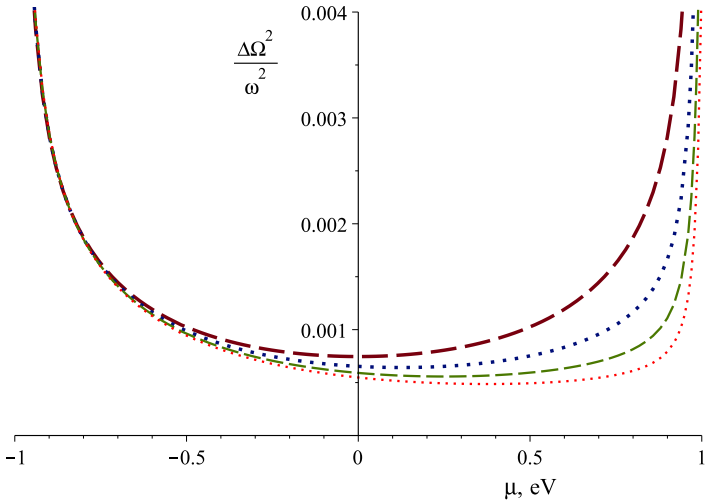

Figure 6. The dependence of $\Delta\Omega^2/\omega^2$ on μ for $U = 3\,eV$ (thick broken line), $3.25\,eV$ (thick dotted line), $3.5\,eV$ (thin broken line), $3.75\,eV$ (thin dotted line) in the case of constant density of states. Parameters: $\kappa = 1$, $\varepsilon_{\min} = -1\,eV$, $\varepsilon_{\max} = 1\,eV$, $\varepsilon_d = -1.5\,eV$, $|\Delta_{\text{sc}}| = 0.02\,eV$.

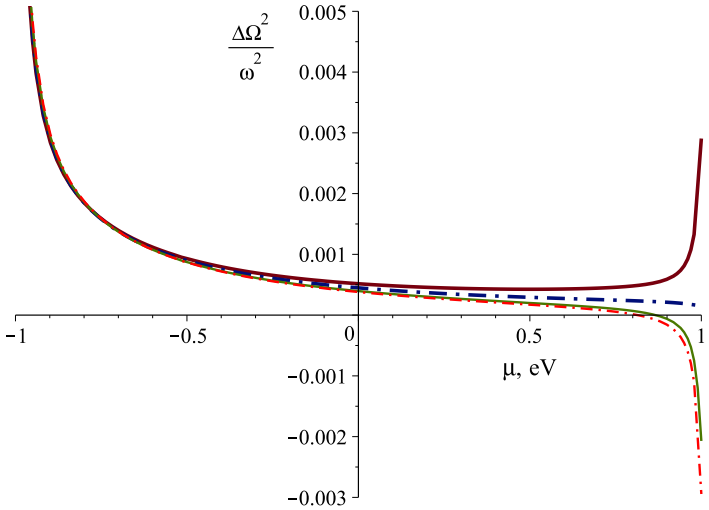

Figure 7. The dependence of $\Delta\Omega^2/\omega^2$ on μ for $U = 4\,eV$ (thick full line), $5\,eV$ (thick chain line), $8\,eV$ (thin full line), $13\,eV$ (thin chain line) in the case of constant density of states. For the rest of the parameters see figure 6

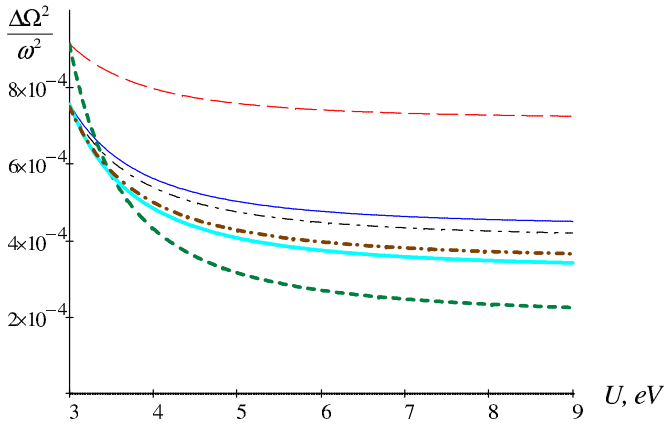

Figure 8. The dependence of $\Delta\Omega^2/\omega^2$ on U for $\mu = -0.4\,eV$ (thin broken line), $-0.1\,eV$ (thin full line), $-0.05\,eV$ (thin chain line), $0.05\,eV$ (thick chain line), $0.1\,eV$ (thick solid line), $0.4\,eV$ (thick broken line) in the case of constant density of states. For the rest of the parameters see figure 3

For the constant density of itinerant electron states, the superconductivity-induced shifts $\Delta\Omega^2/\omega^2$ *vs* chemical potential position calculated on the basis of Eqs. (12) and (10) are shown in figures 6, 7 for various values of U. As expected, the rapid change of $\Delta\Omega^2/\omega^2$ if chemical potential passes through the middle of the band of itinerant electrons is absent in the present case. The hardening of phonon frequency induced by superconductivity is suppressed by the increase of U more substantially in the domain $\mu > 0$. If chemical potential approaches the top of the band of itinerant electrons the effect of softening appears for sufficiently large values of U (thin full line and thin chain line in figure 7). Figure 8 demonstrates the decreasing dependence of $\Delta\Omega^2/\omega^2$ *vs* U for the various positions of chemical potential (c.f. figure 5).

5. Summary

• The impact of electron energy gap formation in the superconducting phase on phonon frequency renormalized by the vibronic mixing of itinerant and localized electron states has been studied.
• If the location of the lower and upper Hubbard levels with regard to the band of itinerant electrons is symmetric or weakly asymmetric, superconductivity induces the hardening of phonon dynamics. The dependence of the effect on μ is stronger near the edges and near the center of conduction band.
• If the location of the Hubbard levels is sufficiently asymmetric, the softening of phonon dynamics appears in certain regions of the chemical potential position.
• For the constant density of electron states the strong dependence of superconductivity-induced shift of phonon frequency on the chemical potential position near the center of conduction band disappears because in this case the van Hove singularity is absent in the center of conduction band.

Acknowledgement

The research was supported by the Estonian Research Council through the Institutional Research Funding IUT2-27 and by the Estonian Science Foundation, Grant No 8991.

References

[1] Testardi L R 1975 *Rev. Mod. Phys.* **47** 637
[2] Plakida 2009 *High Temperature Superconductors* (Heidelberg: Springer)

[3] Vojta M 2009 *Adv. Phys.* **58** 699
[4] Zeyher R and Zwicknagel G 1988 *Solid State Commun.* **66** 617
[5] Zeyher R and Zwicknagel G 1990 *Z. Phys. B - Condensed Matter* **78** 175
[6] Nicol E J, Jiang C and Carbotte J P 1993 *Phys. Rev. B* **47** 8131
[7] Bill A, Hizhnyakov V and Sigmund E 1995 *Phys. Rev. B* **52** 7637
[8] Örd T and Kristoffel N 1997 *Z. Physik. Chemie* **201** 167
[9] Kristoffel N 1990 *phys. stat. sol. (b)* **160** K93
[10] Kristoffel N and Örd T 1991 *Fiz. Nizk. Temp.* **17** 1218; 1991 *Sov. J. Low Temp. Phys.* **17** 641
[11] Bersuker I B 2006 *The Jahn-Teller Effect* (Cambridge: Cambridge University Press)
[12] Kristoffel N and Konsin P 1988 *phys. stat. sol. (b)* **149** 11
[13] Schrieffer J R and Wolff P A 1966 *Phys. Rev.* **149** 491
[14] Zaanen J and Oleś A M 1988 *Phys. Rev. B* **37** 9423
[15] Mattheiss L F and Hamann D R 1989 *Phys. Rev. B* **40** 2217
[16] Emery V J 1987 *Phys. Rev. Lett.* **58** 2794
[17] Hirsch J E 1987 *Phys. Rev. Lett* **59** 228